

LOW-FREQUENCY SOLUTION FOR A PERFECTLY CONDUCTING SPHERE IN A CONDUCTIVE MEDIUM WITH DIPOLAR EXCITATION

P. Vafeas

Division of Applied Mathematics
Department of Chemical Engineering,
University of Patras and ICE/HT-FORTH
GR 265 04 Patras, Greece

G. Perrusson and D. Lesselier

Département de Recherche en Électromagnétisme
Laboratoire des Signaux et Systèmes (CNRS-SUPÉLEC-UPS)
Plateau de Moulon, 91192 Gif-sur-Yvette Cedex, France

Abstract—This contribution concerns the interaction of an arbitrarily orientated, time-harmonic, magnetic dipole with a perfectly conducting sphere embedded in a homogeneous conductive medium. A rigorous low-frequency expansion of the electromagnetic field in positive integral powers $(jk)^n$, k complex wavenumber of the exterior medium, is constructed. The first $n = 0$ vector coefficient (static or Rayleigh) of the magnetic field is already available, so emphasis is on the calculation of the next two nontrivial vector coefficients (at $n = 2$ and at $n = 3$) of the magnetic field. Those are found in closed form from exact solutions of coupled (at $n = 2$, to the one at $n = 0$) or uncoupled (at $n = 3$) vector Laplace equations. They are given in compact fashion, as infinite series expansions of vector spherical harmonics with scalar coefficients (for $n = 2$). The good accuracy of both in-phase (the real part) and quadrature (the imaginary part) vector components of the diffusive magnetic field are illustrated by numerical computations in a realistic case of mineral exploration of the Earth by inductive means. This canonical representation, not available yet in the literature to this time (beyond the static term), may apply to other practical cases than this one in geoelectromagnetics, whilst it adds useful reference results to the already ample library of scattering by simple shapes using analytical methods.

- 1 Context of the Investigation**
- 2 Main Ingredients of the Low-Frequency Scattering Model**
- 3 Specialization to the Spherical Case**
 - 3.1 The Field (Potential) Problems at $n = 0$ and $n = 3$
 - 3.2 The Field Problem at $n = 2$
 - 3.2.1 Enforcing the Divergence Free Property of the Total Magnetic Field
 - 3.2.2 Enforcing the Magnetic Field Boundary Condition on the Sphere Surface
 - 3.2.3 Enforcing the Electric Field Boundary Condition on the Sphere Surface
 - 3.3 The Full Expressions of the Magnetic and Electric Field Coefficients
- 4 Numerical Illustrations**
- 5 Conclusion**
- Appendix A. The Vector Spherical Harmonics and Associated Material**
- References**

1. CONTEXT OF THE INVESTIGATION

In present-day Earth's subsurface electromagnetic probing, especially in mineral exploration, one is often faced with the challenge to retrieve an anomaly of some sort, such as metallic ores, from 3-component magnetic fields measured along a borehole when a low-frequency time-harmonic source is operated nearby, either fixed (usually) at the surface of the Earth or moved (at best) in the same or another borehole. That is, by deciphering such data, orientations, sizes, shapes, electric parameters of the anomalies must be retrieved. However, this inversion task cannot be led in robust fashion unless proper models of the field interaction are available in order to bring good insight to the field behavior and to make available elementary bricks of an inversion algorithm.

Computationally involved 3-D modeling codes are evidently available to that purpose, and one might refer to [1] as a good first example whilst many complementary investigations are found in [2]. But simple methodologies remain useful, as is exemplified early on by

the classical book of [3]. A recent and detailed contribution by [4] (see also references therein) illustrates this type of approach.

The strong electromagnetic and geometric complexity of the Earth, the variety of source-receiver configurations, the need to separate primary fields (hypothetically observed in the absence of the anomalies) and secondary fields due to these anomalies, and the fact that only simplified shapes can effectively be retrieved at the low frequencies employed in such an exploration [†] are some of the reasons that explain the continuing interest in mathematically sound, hopefully robust yet computationally simple modeling tools of the electromagnetic interaction.

In order to put such tools together, the authors and colleagues have advocated working within the framework of the well-known low-frequency scattering theory [5], i.e., by expanding the electromagnetic field in positive integral powers $(jk)^n$, k complex wavenumber of the embedding medium at the operation frequency ω , and by appropriately calculating the vector field coefficients at each n .

Furthermore, they have been suggesting to focus onto the case of a homogeneous conductive triaxial (general) ellipsoid —possibly degenerated to prolate and oblate spheroids or to a sphere— in an Earth-like conductive homogeneous medium, illuminated by an arbitrarily orientated and arbitrarily located time-harmonic magnetic dipole (as a good model of a small electric current loop).

Indeed, in mineral exploration, it is already quite an achievement to show that an orebody behaves as such an ellipsoid, and to accordingly retrieve its geometry and conductivity, by ensuring that the magnetic fields effectively collected along a borehole for a source operated at a few frequencies are close enough to the fields computed for this equivalent ellipsoid; this is argued at length already in [6].

Then, low-contrast cases (say, a ratio between the conductivity, σ_b , of the body and the one, σ , of the medium of less than about 100) can be approached by hybrid means from volumetric Green-based integral formulations of the field conveniently approximated [7] and from expansions of the Green function inside them and of the resulting fields [6, 8].

High-contrast cases (say, with conductivity ratios σ_b/σ well beyond 10^3 , values of 10^5 and more being frequently observed with metallic ores in a resistive Earth) are approximated via the introduction of perfectly conducting (impenetrable) bodies, and the scattering problem is transformed into a succession, one at each n ,

[†] Up to a few kHz, distances between sources and receivers and anomalies and the dimensions of the anomalies are a fraction of the plane-wave skin depth in a subsoil the conductivity of which usually ranges between a few mS/m and a few tens mS/m.

of possibly coupled boundary value problems formulated according to second-order partial differential equations (Laplace) with proper perfectly reflecting boundary conditions, and closed-form solutions thereof, the latter being expanded accordingly by using available solid or vector harmonics [9] in the ellipsoidal or degenerate system of coordinates which is attached to the body [10].

However, to reach these representations of the field even in the canonical configuration is not straightforward in view of the localized vector sources (instead of plane waves), the near fields (instead of far fields) and the conductive embedding media (instead of vacuum) that are to be dealt with; for the most part closed-form results appear still absent from the literature on scattering by simple shapes to the best of our knowledge.

That is, the expectedly standard static, $n = 0$ coefficient (Rayleigh) of the secondary magnetic field—which is the one that would be observed for a dipolar excitation of an ellipsoid in vacuum satisfying a Neumann boundary condition—appears to have been proposed for the first time in [10] using expansions in solid ellipsoidal harmonics up to degree 3 (the harmonics of higher degree are not known in explicit fashion) of the scalar potential. Let us notice that the spherical case is considered in this paper [10] as well, now using expansions in solid spherical harmonics up to arbitrary degree; yet no claim was made for their originality (being said we do not know of any reference in the open literature where these expansions would be given in full). ‡

As for the next coefficients (for the dipolar illumination they will be nontrivial from $n = 2$ as shown in section 2), henceforth termed as dynamic ones since they contribute to the imaginary part (quadrature) of the magnetic field in addition to possibly contributing to its real part (in-phase), and involve the perturbation of conduction currents in the embedding medium induced by the given source (both galvanic and vortex effects are modeled here), the ellipsoidal case is not treated anywhere.

Even, the low-frequency expansions in the spherical case are not available, again to the best of our knowledge. Results are available for a penetrable sphere illuminated by a dipolar magnetic field within a conductive host medium via a Mie series expansion [7], possible low-frequency counterparts being not exploited however. In [3] a low-frequency expansion is found by the clever manipulation of Debye potentials, but the approach does not accommodate for a perfectly

‡ In [10], part of the investigation is devoted to identification of a spherical or ellipsoidal orebody from synthetic data as well as from real data acquired in the field, which identification problem is not considered in the present contribution.

conducting sphere via an asymptotic analysis.

Here, one will limit ourselves to the sphere case, with most emphasis on the $n = 2$ vector coefficient (the $n = 3$ is easier to get again as the gradient of a scalar potential), as a preliminary yet necessary example of the interest of the method. This, in addition to the interest for practical applications, like mining exploration here, or so-called UnExploded Ordinance (UXO) investigations [11] or like the exploration of natural structures such as water-filled cavities and other possibly conductive anomalies in subsoil at shallow depths, will be adding what is believed to be useful reference results to the already ample library of scattering by simple shapes using analytical methods [12, 13].

Let us emphasize that a difficult and cumbersome work on the dynamic terms in the general ellipsoidal case is still not fully completed at the present time [14]. However, the lack of high degree ellipsoidal harmonics implies that even a clever degeneracy of the ellipsoidal formulas to the spherical ones fails to reproduce the full spherical representation as is exemplified already in [10] for the Rayleigh term, but should yield a few of the contributors to each n coefficient only. So, the sphere analysis carried out herein is valuable *per se*.

Also, the proposed approach makes good use of the external vector spherical harmonics for the Laplace equation. Indeed, they enable us to express the unknown field coefficients as a sum of series expansions involving vector harmonics with scalar coefficients, instead of expressing them as a sum of series expansions involving solid spherical harmonics with 3-component vector coefficients. This leads to far less unknowns (three times less), provides for rather elegant calculations, and results into compact formulas —notice that neither the ellipsoidal case nor the spheroidal ones enjoy explicit knowledge of all needed vector harmonics, which, for such geometries, would force us to take the long way via calculation of many scalar factors.

The paper itself is organized as follows. After this rather long yet believed to be necessary analysis of the context in this section, one sketches in section 2 the low-frequency analysis as specialized to the scattering by a 3-D bounded, impenetrable smooth body in a conductive host medium illuminated by a magnetic dipole. Then, in Section 3, one describes the main steps that enable us to handle the sphere case, focusing onto the novel material (the $n = 2$ and at a much lesser degree of complexity the $n = 3$ coefficients). In Section 4 one illustrates these results by numerical examples in a realistic mining exploration case. A short outline of forthcoming works follows. In Appendix, key elements on the vector spherical harmonics are reminded for completeness.

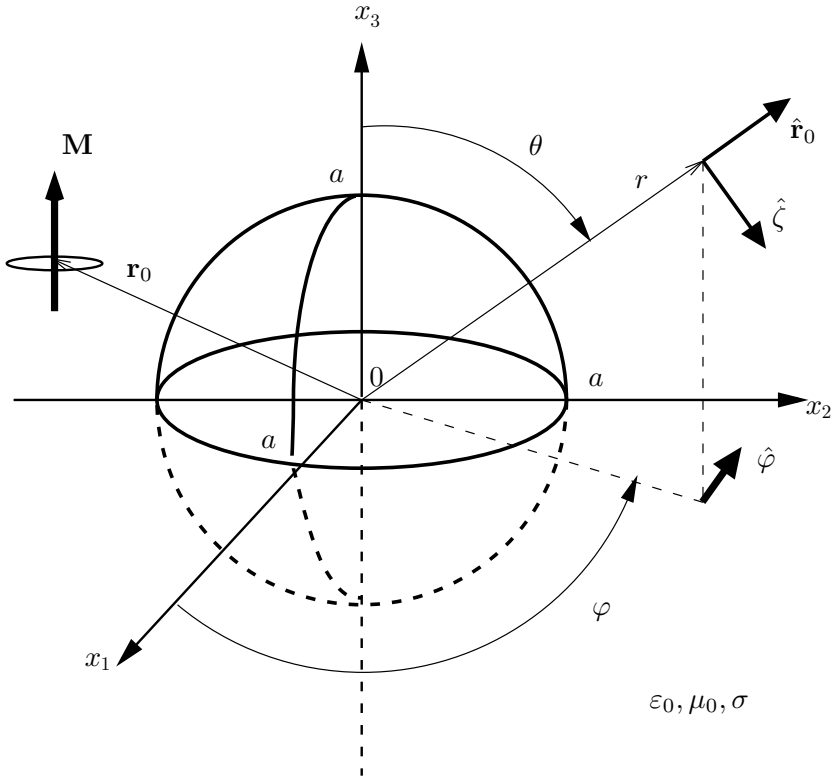


Figure 1. A perfectly conductive a radius sphere, placed at the center O of Cartesian co-ordinate system (x_1, x_2, x_3) , in a non-magnetic (permeability μ_0) conductive (σ) medium, is illuminated by a magnetic dipole \mathbf{M} orientated along the x_3 axis and localized in \mathbf{r}_0 . (r, θ, φ) represents a spherical co-ordinate system, and $(\hat{\mathbf{r}}, \hat{\zeta}, \hat{\varphi})$ —where $\zeta = \cos(\theta)$ —are unit vectors of this system.

2. MAIN INGREDIENTS OF THE LOW-FREQUENCY SCATTERING MODEL

The ingredients of the model put forth can be summarized as follows (here, taking good part of the material from [10]) with reference to the geometry in Figure 1 (here drawn for a spherical body, for simplicity and in accord with the investigation pursued later on).

Let $k = (j\omega\sigma\mu_0)^{1/2}$ (or correspondingly $k = (1 + j)/\delta$, δ planar skin depth) be the wavenumber at low circular frequency ω (with

henceforth implied time-dependence $\exp(-j\omega t)$ in the linear isotropic, non-magnetic (permeability μ_0) conductive host medium (conductivity σ); polarization effects are assumed to be negligible at this stage, only conduction currents flow inside the medium.

A magnetic dipole \mathbf{M} with orientation taken along the \mathbf{x}_3 axis of a set of Cartesian co-ordinates (this does not reduce the generality of the analysis) and amplitude $M = 4\pi$ is operated at location \mathbf{r}_0 .

A single voluminous anomaly Ω with smooth boundary contour (it will be specialized to a sphere of radius a in section 3) whose conductivity σ_b is large enough with respect to the background one to be assumed as of infinite value, is also contained inside the conductive host medium. The primary electromagnetic field $(\mathbf{E}^P, \mathbf{H}^P)$ radiated in the medium interacts with the body, which gives birth to a secondary electromagnetic field $(\mathbf{E}^S, \mathbf{H}^S)$ the magnetic field of which is collected (via a 3-component probe) at some \mathbf{r} (typically along a single line \mathcal{L} passing outside the body).

Now, one is interested in vector series expansions in positive integral powers $(jk)^n$ of the electromagnetic field, e.g., expansions of the form $\mathbf{U} = \sum_n \mathbf{U}_n(jk)^n$, \mathbf{U}_n real-valued and independent of k , the integer n running from 0 to ∞ —which low-frequency series expansions are known to converge for k small enough [5].

The primary fields at \mathbf{r} due to the magnetic dipole at \mathbf{r}_0 enjoy such expansions (implying \mathbf{r} hereafter):

$$\mathbf{E}^P = \mathbf{E}_2^P(jk)^2 + O(jk)^4, \quad (1)$$

$$\mathbf{H}^P = \mathbf{H}_0^P + \mathbf{H}_2^P(jk)^2 + \mathbf{H}_3^P(jk)^3 + O(jk)^4. \quad (2)$$

The electric and magnetic field coefficients at $n = 4$ are nonzero, but they are not considered further on.[§] Using dyadic notations via underlining of the concerned quantity, letting $\underline{\mathbf{I}}$ be the identity dyad, and upon introduction of $\mathbf{R} = \mathbf{r} - \mathbf{r}_0$ and $R = |\mathbf{r} - \mathbf{r}_0|$, magnetic and electric vector coefficients readily follow:

$$\mathbf{H}_0^P = \frac{1}{R^3} \left[\frac{3\mathbf{R}\mathbf{R}}{R^2} - \underline{\mathbf{I}} \right] \cdot \mathbf{x}_3 = \nabla \left[\frac{1}{R} \right] \cdot \mathbf{x}_3 \quad (3)$$

$$\mathbf{H}_2^P = -\frac{1}{2R} \left[\frac{\mathbf{R}\mathbf{R}}{R^2} + \underline{\mathbf{I}} \right] \cdot \mathbf{x}_3 = -\frac{1}{2} \left[-(\nabla \frac{1}{R})\mathbf{R} + \frac{\underline{\mathbf{I}}}{R} \right] \cdot \mathbf{x}_3 \quad (4)$$

$$\mathbf{H}_3^P = -\frac{2}{3}\mathbf{x}_3, \quad (5)$$

[§] Let us notice that if the host medium is not modeled as purely conductive, say, if some polarization effects are introduced in view of a possibly high operation frequency (nearing 1 MHz in the context of subsoil exploration) via a real-valued permittivity ϵ , this would only affect elements at order $n = 4$ and beyond.

$$\mathbf{E}_2^P = -\frac{1}{\sigma} \mathbf{x}_3 \times \frac{\mathbf{R}}{R^3} = \frac{1}{\sigma} \mathbf{x}_3 \times \nabla \frac{1}{R}. \quad (6)$$

Let us notice that magnetic terms of order n vary like $1/R^{3-n}$ and the electric ones vary like $1/R^{4-n}$ when range R increases to infinity.

By insertion of the series expansions of the secondary fields within the Maxwell's PDE which these fields satisfy, and by taking into account the triviality of several primary field coefficients above, one obtains first-order differential relationships for the nontrivial coefficients up to order 3 as

$$\nabla \times \mathbf{H}_0^S = \mathbf{0}, \quad (7)$$

$$\nabla \times \mathbf{E}_2^S = -\frac{1}{\sigma} \mathbf{H}_0^S \quad (8)$$

$$\nabla \times \mathbf{H}_2^S = \sigma \mathbf{E}_2^S, \quad (9)$$

$$\nabla \times \mathbf{H}_3^S = \mathbf{0}, \quad (10)$$

all field coefficients being divergence free.

As for the perfectly reflecting boundary conditions at the body surface, i.e., cancellation of the normal component of the magnetic field and cancellation of the tangential component of the electric field, they apply at each order n . One has

$$[\mathbf{H}_n^P + \mathbf{H}_n^S] \cdot \mathbf{n} = 0, \quad (11)$$

$$[\mathbf{E}_n^P + \mathbf{E}_n^S] \times \mathbf{n} = \mathbf{0}, \quad (12)$$

where \mathbf{n} is the unit exterior normal.

Equivalently to the above first-order differential equations and boundary conditions, the static ($n = 0$) coefficient of the secondary magnetic field (the one of the electric field is zero) is the solution of a standard potential problem in vacuum with Neumann boundary condition:

$$\mathbf{H}_0^S = \nabla \Phi_0^S, \quad \Delta \Phi_0^S = 0, \quad \partial_n \Phi_0^S = -\partial_n \Phi_0^P, \quad (13)$$

letting Φ_0^P the primary potential, with normal derivative denoted as ∂_n . A similar relationship holds true with the third, $n = 3$ coefficient of the secondary magnetic field, once replaced the primary potential by the proper one, Φ_3^P , here associated to a coefficient uniform throughout space.

As for the $n = 2$ coefficient of the secondary magnetic field, from the above, it is easily seen that it satisfies the inhomogeneous vector Laplace equation

$$\Delta \mathbf{H}_2^S = \mathbf{H}_0^S \quad (14)$$

with vector Laplacian Δ , the boundary conditions being still to be enforced.

For cases $n = 0$ and $n = 3$ it will suffice to calculate scalar potentials, which is not expected to be a considerable task in a system of coordinates attached to a canonical body (e.g., an ellipsoid and degenerate shapes) for which solid harmonics as solutions of the homogeneous scalar Laplace equation are available (at least to an extent, e.g., the ellipsoidal geometry), which enables us to expand the unknown coefficients onto them.

At $n = 2$, the mathematical formulation (14) looks at first hand more complicated. But the vector biharmonic coefficient \mathbf{H}_2^S writes down as the sum of a particular solution, henceforth denoted as \mathbf{H}_2^{Spar} , of this inhomogeneous equation (14) and of a general vector harmonic solution, henceforth denoted as \mathbf{H}_2^{Sgen} , of the corresponding homogeneous equation. Since $\mathbf{H}_0^S = \nabla\Phi_0^S$, standard vector algebra (in particular $\Delta\mathbf{r} = \mathbf{0}$) enables us to exhibit as a particular solution the purely radial function

$$\mathbf{H}_2^{Spar} = \frac{1}{2}\Phi_0^S\mathbf{r}, \quad (15)$$

the electric field coefficient being

$$\mathbf{E}_2^{Spar} = \frac{1}{2\sigma}\nabla\Phi_0^S \times \mathbf{r}. \quad (16)$$

So, there mostly remains to tackle the homogeneous equation, again profiting from the fact that the previous solid harmonics, or, better, the vector harmonics as solutions of the homogeneous vector Laplace equation, may be available in order to expand the unknown field coefficients onto them.

3. SPECIALIZATION TO THE SPHERICAL CASE

Let us now specialize the analysis to a sphere of radius a centered at the center of coordinates O . This requires first a reminder of material on solid and vector spherical harmonics [15, 9]; this material is given in Appendix A. One will heavily draw from it in the next two subsections, referring to specific relationships of the Appendix A only in special cases.

3.1. The Field (Potential) Problems at $n = 0$ and $n = 3$

As already said, at orders $n = 0$ (static) and $n = 3$, one simply has to solve potential problems (results have already been given, in part, in the first case [10]).

As given in the above, the static primary potential associated to the field coefficient in (3) enjoys a very simple expression, $\Phi_0^P(\mathbf{r}) = \nabla(\frac{1}{R}) \cdot \mathbf{x}_3$. The expansion of the inverse distance on the solid harmonics is well known. For $r < r_0$,

$$\frac{1}{R} = \sum_{n=0}^{\infty} \frac{r^n}{r_0^{n+1}} \sum_{m=0}^n \frac{(n-m)!}{(n+m)!} \varepsilon_m P_n^m(\zeta) P_n^m(\zeta_0) \cos[m(\varphi - \varphi_0)], \quad (17)$$

where $\zeta = \cos \theta$, $\zeta_0 = \cos \theta_0$, $\varepsilon_0 = 1$, and $\varepsilon_{m \neq 0} = 2$, the P_n^m being the associated Legendre polynomials.

Matching the magnetic boundary condition at the surface $r = a$ of the sphere (i.e., cancellation of the normal derivative of the total potential) yields the secondary magnetic potential as a multipole expansion:

$$\begin{aligned} \Phi_0^S(\mathbf{r}) = & \sum_{n=0}^{\infty} \frac{a^{2n+1}}{r^{n+1} r_0^{n+2}} \sum_{m=0}^n \frac{(n-m+1)!}{(n+m)!} \\ & \cdot \varepsilon_m \frac{n}{(n+1)} P_{n+1}^m(\zeta_0) P_n^m(\zeta) \cos[m(\varphi - \varphi_0)]. \end{aligned} \quad (18)$$

The magnetic field coefficient immediately results from a gradient operation:

$$\mathbf{H}_0^S(\mathbf{r}) = - \sum_{n=1}^{\infty} \frac{a^{2n+1}}{r^{n+2} r_0^{n+2}} \sum_{m=0}^n \frac{(n-m+1)!}{(n+m)!} \varepsilon_m \frac{n}{(n+1)} P_{n+1}^m(\zeta_0) \mathbf{f}_n^m. \quad (19)$$

In the attached spherical coordinate system (centered at the sphere center, with unit vectors $\hat{\mathbf{r}}, \hat{\zeta}, \hat{\varphi}$), the three components of the range-independent vector coefficients \mathbf{f}_n^m are

$$\begin{aligned} f_n^m|_r &= (n+1) P_n^m(\zeta) \cos[m(\varphi - \varphi_0)], \\ f_n^m|_{\zeta} &= \sqrt{1 - \zeta^2} P_n^{m'}(\zeta) \cos[m(\varphi - \varphi_0)], \\ f_n^m|_{\varphi} &= \frac{1}{\sqrt{1 - \zeta^2}} m P_n^m(\zeta) \sin[m(\varphi - \varphi_0)]. \end{aligned} \quad (20)$$

where the prime indicates derivation with respect to the argument.

At $n = 3$, one can in effect bypass the calculation of the primary potential, the value of the secondary field being derived almost per inspection. Indeed the primary field is a constant vector, as $\mathbf{H}_3^P(\mathbf{r}) = -\frac{2}{3} \mathbf{x}_3$. So, its projection onto the normal at the sphere surface $r = a$ has the only angular dependance $\zeta = \cos \theta$, which is none other than the even scalar surface harmonic of order 0 and degree 1, Y_1^{0e} . Since

the secondary field (the gradient of a potential) should have the general form $\mathbf{H}_3^S(\mathbf{r}) = \sum_{n=0}^{\infty} \sum_{m=0}^n \sum_{s=e,o} S_n^{ms} \left(\nabla \frac{1}{r^{n+1}} Y_n^m(\hat{\mathbf{r}}) \right)$, cancellation of the sum of the primary and secondary field components normal to the surface involves that all sought coefficients S_n^{ms} are trivial, save S_1^{0e} which is the only one to bring out the proper cosine dependance (this coefficient calculates as $-\frac{a^3}{3}$). Finally, one arrives at the very simple result

$$\mathbf{H}_3^S(\mathbf{r}) = \frac{1}{3} \left(\frac{a}{r} \right)^3 \left[2\zeta \hat{\mathbf{r}} + \sqrt{1 - \zeta^2} \hat{\zeta} \right]. \quad (21)$$

3.2. The Field Problem at $n = 2$

As shown in the previous section, the magnetic field coefficient at order $n = 2$ is made of a particular radial solution, \mathbf{H}_2^{Spar} , as given in (15) and of a general vector harmonic solution, \mathbf{H}_2^{Sgen} .

The particular solution is considered from (18). After some standard manipulations that enable us to introduce a summation of even and odd surface harmonics $Y_n^{ms}(\hat{\mathbf{r}})$, one finds

$$\mathbf{H}_2^{Spar}(\mathbf{r}) = \sum_{n=0}^{\infty} \sum_{m=0}^n \sum_{s=e,o} A_n^{ms} r^{-n} Y_n^{ms}(\hat{\mathbf{r}}) \hat{\mathbf{r}}, \quad (22)$$

where one has let

$$A_n^{ms} = \frac{1}{2} \frac{(n-m)!}{(n+m)!} \varepsilon_m \frac{a^{2n+1}}{r_0^{n+2}} \frac{n(n-m+1)}{(n+1)} P_{n+1}^m(\zeta_0) \begin{cases} \cos m\varphi_0, & s = e \\ \sin m\varphi_0, & s = o \end{cases}. \quad (23)$$

The transverse electric field coefficient \mathbf{E}_2^{Spar} follows as

$$\mathbf{E}_2^{Spar}(\mathbf{r}) = \frac{1}{\sigma} \sum_{n=1}^{\infty} \sum_{m=0}^n \sum_{s=e,o} A_n^{ms} \mathbf{M}_n^{ms}(\mathbf{r}) \quad (24)$$

by readily using the definition of the \mathbf{M}_n^{ms} vector harmonic in (A11).

The general solution, according to the expansion (A15), is expressed as

$$\begin{aligned} \mathbf{H}_2^{Sgen}(\mathbf{r}) &= \sum_{n=1}^{\infty} \sum_{m=0}^{n-1} \sum_{s=e,o} a_n^{ms} \mathbf{N}_n^{ms}(\mathbf{r}) + \sum_{n=1}^{\infty} \sum_{m=0}^n \sum_{s=e,o} b_n^{ms} \mathbf{M}_n^{ms}(\mathbf{r}) \\ &+ \sum_{n=0}^{\infty} \sum_{m=0}^{n+1} \sum_{s=e,o} c_n^{ms} \mathbf{G}_n^{ms}(\mathbf{r}). \end{aligned} \quad (25)$$

Consequently, in view of the curl relationships satisfied by the vector harmonics and after a shift of the n index in the second summation, one has

$$\mathbf{E}_2^{Sgen}(\mathbf{r}) = \frac{1}{\sigma} \left[- \sum_{n=1}^{\infty} \sum_{m=0}^n \sum_{s=e,o} nb_n^{ms} \mathbf{N}_{n+1}^{ms}(\mathbf{r}) + \sum_{n=1}^{\infty} \sum_{m=0}^n \sum_{s=e,o} (2n-1) c_{n-1}^{ms} \mathbf{M}_n^{ms}(\mathbf{r}) \right]. \quad (26)$$

The three sets $\{a_n^{ms}\}$, $\{b_n^{ms}\}$, $\{c_n^{ms}\}$, of scalar coefficients introduced above have to be constructed in accord with the primary field data, with the value of the particular solution, and with the boundary conditions. The procedure is considered below, only the main steps being emphasized in view of the large amount of calculations to be performed.

3.2.1. Enforcing the Divergence Free Property of the Total Magnetic Field

The first obvious step is to enforce that the total magnetic field component is divergence free. Doing so provides us with the $\{c_n^{ms}\}$ set of coefficients since the two other sets, $\{a_n^{ms}\}$ and $\{b_n^{ms}\}$, are coefficients of vector harmonics that are divergence free.

The divergence of the general solution immediately follows from the material in Appendix as

$$\nabla \cdot \mathbf{H}_2^{Sgen}(\mathbf{r}) = \sum_{n=0}^{\infty} \sum_{m=0}^{n+1} \sum_{s=e,o} [-(n+1)(2n+1)] r^{-(n+2)} c_n^{ms} Y_{n+1}^{ms}(\hat{\mathbf{r}}). \quad (27)$$

As for the divergence of the particular solution, it is valued at $\frac{1}{2}(3\Phi_0^S + \mathbf{H}_0^S \cdot \mathbf{r})$ from (15). After proper introduction of even and odd surface harmonics so as the general and particular solutions look alike, it reads as

$$\nabla \cdot \mathbf{H}_2^{Spar}(\mathbf{r}) = \sum_{n=0}^{\infty} \sum_{m=0}^{n+1} \sum_{s=e,o} [-(n-1)A_{n+1}^{ms}] r^{-(n+2)} Y_{n+1}^{ms}(\hat{\mathbf{r}}). \quad (28)$$

The sum of the two divergences should be null everywhere, which implies that all resulting coefficients of the harmonics $Y_{n+1}^{ms}(\hat{\mathbf{r}})$ cancel out, i.e., one finds

$$c_n^{ms} = -\frac{(n-1)}{(n+1)(2n+1)} A_{n+1}^{ms}, n = 0, 1, \dots; m = 0, 1, \dots, n+1; s = e, o. \quad (29)$$

Detailed expressions of the corresponding set of coefficients, $\{c_n^m\}$, where the sine or cosine parts are taken off, are regrouped at the end of the subsection with all others involved.

Now, let us consider the satisfaction of the boundary conditions. First one has to obtain proper expansions of the primary magnetic and electric field coefficients at the sphere surface $r = a$, as well as of the particular solution. Here, let us emphasize that one will only need (for example) the normal (radial) components of $\hat{\mathbf{r}} \cdot \mathbf{H}_2^P$ and $\hat{\mathbf{r}} \cdot \mathbf{H}_2^{Spar}$, of the magnetic one, and only one of the two tangential components of $\hat{\mathbf{r}} \times \mathbf{E}_2^P$ and $\hat{\mathbf{r}} \times \mathbf{E}_2^{Spar}$ of the electric one, since only two sets of coefficients remain to be calculated, and two sets of equations are sufficient to do so.

3.2.2. Enforcing the Magnetic Field Boundary Condition on the Sphere Surface

From the second expression of the primary magnetic field coefficient \mathbf{H}_2^P in the right-hand side of (4), its radial component reads in detailed form as

$$\hat{\mathbf{r}} \cdot \mathbf{H}_2^P(\mathbf{r}) = \frac{1}{2} \left[(a\zeta - r_0\zeta_0) \frac{\partial}{\partial r} \frac{1}{|r - r_0|} \Big|_{r=a} - \zeta \frac{1}{|r - r_0|} \Big|_{r=a} \right]. \quad (30)$$

From the expansion (17) of the inverse distance $\frac{1}{|r - r_0|}$ and accounting for the recurrence relationships satisfied by the associated Legendre polynomials P_n^m and their derivatives, after suitably regrouping the several terms obtained in this way, one gets

$$\hat{\mathbf{r}} \cdot \mathbf{H}_2^P(r) \Big|_{r=a} = \frac{1}{2} \sum_{n=0}^{\infty} \sum_{m=0}^n \frac{(n-m)!}{(n+m)!} \varepsilon_m \frac{a^n}{r_0^{n+1}} \alpha_n^m P_n^m(\zeta) \cos(m(\varphi - \varphi_0)) \quad (31)$$

letting the intermediary coefficient α_n^m , from $n = 0$ for $m = 0, 1, \dots, n$, be

$$\begin{aligned} \alpha_n^m &= -\frac{r_0}{a} \frac{2(n+1)(n+m)}{(2n-1)(2n+1)} P_{n-1}^m(\zeta_0) \\ &\quad + n(n-m+1) \left[\frac{a}{r_0} \frac{1}{2n+3} - \frac{r_0}{a} \frac{1}{2n+1} \right] P_{n+1}^m(\zeta_0), \end{aligned} \quad (32)$$

noticing that $\alpha_0^0 = 0$. After some further manipulation the sought surface harmonic expansion of the radial component of the primary magnetic field coefficient becomes

$$\hat{\mathbf{r}} \cdot \mathbf{H}_2^P(\mathbf{r}) \Big|_{r=a} = \sum_{n=0}^{\infty} \sum_{m=0}^n \sum_{s=e,o} \Omega_n^{ms} Y_n^{ms}(\hat{\mathbf{r}}), \quad (33)$$

where one has introduced for brevity

$$\Omega_n^{ms} = \Omega_n^m \begin{cases} \cos m\varphi_0, & s = e \\ \sin m\varphi_0, & s = o \end{cases}, \quad (34)$$

the value of Ω_n^m being easily derived from the preceding relationships as

$$\Omega_n^m = \frac{1}{2} \frac{(n-m)!}{(n+m)!} \varepsilon^m \frac{a^n}{r_0^{n+1}} \alpha_n^m. \quad (35)$$

At the same time working on the particular solution brings out

$$\hat{\mathbf{r}} \cdot \mathbf{H}_2^{Spar}(\mathbf{r}) \Big|_{r=a} = \sum_{n=0}^{\infty} \sum_{m=0}^n \sum_{s=e,o} A_n^{ms} a^{-n} Y_n^{ms}(\hat{\mathbf{r}}). \quad (36)$$

Now, cancellation of the normal magnetic field coefficient at $r = a$ directly provides us with the a_n^{ms} coefficients. Indeed, the b_n^{ms} coefficients in (25) are factors of purely transverse harmonics \mathbf{M}_n^{ms} , whilst the c_n^{ms} coefficients—which are associated to some radial contribution as well—are already available. Since one knows from (A13) and (A14) the radial components of the \mathbf{N}_n^{ms} and \mathbf{G}_n^{ms} versus the Y_n^{ms} surface harmonics, cancelling out the sum of the several coefficients of Y_n^{ms} at each involved n within the expression of the total normal component yields coefficients a_n^{ms} which satisfy

$$na^{-(n+1)} a_n^{ms} = \Omega_{n-1}^{ms} + a^{-(n-1)} A_{n-1}^{ms} + (n-1)a^{-(n-1)} c_{n-2}^{ms}, \\ n = 1, 2, \dots; m = 0, 1, \dots, n-1; s = e, o. \quad (37)$$

Let us notice that a_1^{0s} is null (the subscript of c in the above may reach -1 , but its factor is identically zero, so it does not matter). Final expressions of the corresponding coefficients a_n^m , where the sine or cosine parts are taken off, follow (they are again given at the end of the subsection).

3.2.3. Enforcing the Electric Field Boundary Condition on the Sphere Surface

Since there remains only the set $\{b_n^m\}$ to be found at this stage, it suffices to cancel out one transverse component of the total electric field coefficient at the sphere surface $r = a$ —if this is done in proper fashion the other transverse component should consequently be zero as well, which is indeed a result one has checked afterwards. Next one has worked with the ζ component. Similarly to the above analysis, from

the second expression of \mathbf{E}_2^P in the right-hand side of (6), after simple yet quite lengthy calculations, one gets

$$\hat{\mathbf{r}} \times \mathbf{E}_2^P(\mathbf{r}) \Big|_{r=a} = \frac{1}{\sigma \sqrt{1-\zeta^2}} \sum_{n=0}^{\infty} \sum_{m=0}^n \frac{(n-m)!}{(n+m)!} \varepsilon_m \left[\frac{a^{n-1}}{r_0^{n+1}} \beta_n^m \sin(m(\varphi - \varphi_0)) \hat{\boldsymbol{\varphi}} + \frac{a^n}{r_0^{n+2}} \gamma_n^m \cos(m(\varphi - \varphi_0)) \hat{\boldsymbol{\zeta}} \right] P_n^m(\zeta), \quad (38)$$

letting intermediary coefficients β_n^m and γ_n^m be

$$\beta_n^m = m \left[\frac{r_0}{a} \frac{(n+m)}{(2n-1)} P_{n-1}^m(\zeta_0) + \frac{a}{r_0} \frac{(n-m+1)}{(2n+3)} P_{n+1}^m(\zeta_0) \right], \quad (39)$$

and

$$\gamma_n^m = -\frac{r_0}{a} \left[\frac{(n+m)(n+m-1)}{(2n-1)} - m \right] P_n^m(\zeta_0) - \frac{a}{r_0} \frac{(n-m+1)(n-m+2)}{(2n+3)} P_{n+2}^m(\zeta_0). \quad (40)$$

After some manipulation of the primary contribution in (38), (39), (40), one gets the general form

$$\hat{\mathbf{r}} \times \mathbf{E}_2^P(\mathbf{r}) \cdot \hat{\boldsymbol{\zeta}} \Big|_{r=a} = \frac{1}{\sigma \sqrt{1-\zeta^2}} \sum_{n=0}^{\infty} \sum_{m=0}^n \sum_{s=e,o} \Gamma_n^{ms} Y_n^{ms}(\hat{\mathbf{r}}), \quad (41)$$

where one has set

$$\Gamma_n^{ms} = \Gamma_n^m \begin{cases} \cos m\varphi_0, & s = e \\ \sin m\varphi_0, & s = o \end{cases}, \quad (42)$$

the value of Γ_n^m being easily derived from the preceding relationships as

$$\Gamma_n^m = \frac{(n-m)!}{(n+m)!} \varepsilon_m \frac{a^n}{r_0^{n+2}} \gamma_n^m. \quad (43)$$

As for the transverse electric part $\mathbf{r} \times \mathbf{E}_2^{Spar}$ of the particular solution, one easily shows that

$$\hat{\mathbf{r}} \times \mathbf{E}_2^{Spar}(\mathbf{r}) \Big|_{r=a} = \frac{1}{\sigma} \sum_{n=1}^{\infty} \sum_{m=0}^n \sum_{s=e,o} A_n^{ms} \sqrt{n(n+1)} a^{-(n+1)} \mathbf{B}_n^{ms}(\hat{\mathbf{r}}). \quad (44)$$

Finally, starting from (26), one arrives at the corresponding transverse part of the general solution as

$$\mathbf{r} \times \mathbf{E}_2^{Sgen}(\mathbf{r}) \Big|_{r=a} = \frac{1}{\sigma} \sum_{n=1}^{\infty} \sum_{m=0}^n \sum_{s=e,o} \sqrt{n(n+1)} a^{-(n+2)} [nb_n^{ms} \mathbf{C}_n^{ms}(\hat{\mathbf{r}}) + (2n-1)ac_{n-1}^{ms} \mathbf{B}_n^{ms}(\hat{\mathbf{r}})]. \quad (45)$$

Since one is able to calculate from (A7), (A8) the transverse components of the \mathbf{B}_n^{ms} and \mathbf{C}_n^{ms} vector surface harmonics as a function of the $Y_n^{ms}(\hat{\mathbf{r}})$ scalar surface harmonics, the problem left here boils down to cancelling out the sum of the several factors of $Y_n^{ms}(\hat{\mathbf{r}})$ within the total ζ -component at $r = a$ derived from the above. Careful book-keeping is especially required in view of the number of terms involved, whilst the even and odd order terms are treated in separate fashion for simplicity and regrouped thereafter. In so doing, one is able to show the following relationship:

$$\begin{aligned} -2a^{-(n+2)} \frac{(n+2)(n+m+1)}{(2n+3)(n+1)} A_{n+1}^{ms} + \frac{2(n-m)}{(2n-1)} a^{-n} A_{n-1}^{ms} \\ + \delta_s m n a^{-(n+2)} b_n^{m\bar{s}} + \Gamma_n^{ms} = 0 \\ n = 1, 2, \dots; m = 0, 1, \dots, n; \delta_{s=e} = 1; \delta_{s=o} = -1; \end{aligned} \quad (46)$$

\bar{s} here means a superscript o if $s = e$ and vice-versa. Detailed expressions of the corresponding coefficients b_n^m , where the sine or cosine parts are taken off, follow (they are given below).

3.3. The Full Expressions of the Magnetic and Electric Field Coefficients

Collecting all previous results as indicated before, with separation of the $m\varphi_0$ sine and cosine contributions for clarity, one has

$$\begin{aligned} \mathbf{H}_2^S(\mathbf{r}) = & \sum_{n=1}^{\infty} \sum_{m=0}^n d_n^m r^{-n} [\cos(m\varphi_0) \mathbf{P}_n^{me}(\hat{\mathbf{r}}) + \sin(m\varphi_0) \mathbf{P}_n^{mo}(\hat{\mathbf{r}})] \\ & + \sum_{n=1}^{\infty} \sum_{m=0}^{n-1} a_n^m [\cos(m\varphi_0) \mathbf{N}_n^{me}(\mathbf{r}) + \sin(m\varphi_0) \mathbf{N}_n^{mo}(\mathbf{r})] \\ & + \sum_{n=1}^{\infty} \sum_{m=0}^n b_n^m [-\sin(m\varphi_0) \mathbf{M}_n^{me}(\mathbf{r}) + \cos(m\varphi_0) \mathbf{M}_n^{mo}(\mathbf{r})] \\ & + \sum_{n=0}^{\infty} \sum_{m=0}^{n+1} c_n^m [\cos(m\varphi_0) \mathbf{G}_n^{me}(\mathbf{r}) + \sin(m\varphi_0) \mathbf{G}_n^{mo}(\mathbf{r})], \end{aligned} \quad (47)$$

and, in accord with divergence and curl relationships satisfied by the harmonics,

$$\begin{aligned} \sigma \mathbf{E}_2^S(\mathbf{r}) = & \sum_{n=1}^{\infty} \sum_{m=0}^n \frac{2}{n} d_n^m [\cos(m\varphi_0) \mathbf{M}_n^{me}(\mathbf{r}) + \sin(m\varphi_0) \mathbf{M}_n^{mo}(\mathbf{r})] \\ & - nb_n^m [-\sin(m\varphi_0) \mathbf{N}_{n+1}^{me}(\mathbf{r}) + \cos(m\varphi_0) \mathbf{N}_{n+1}^{mo}(\mathbf{r})]. \end{aligned} \quad (48)$$

The four sets of scalar coefficients involved in the above are given by

$$\begin{aligned} d_n^m &= \frac{1}{2} \frac{(n-m)!}{(n+m)!} \varepsilon_m \frac{n(n-m+1)}{(n+1)} \frac{a^{2n+1}}{r_0^{n+2}} P_{n+1}^m(\zeta_0) \\ a_n^m &= \frac{(n-m)!}{(n+m)!} \varepsilon_m \frac{(n+m)}{n(n-m)} \left[-\frac{a^{2n-1}}{r_0^{n-1}} \frac{n(n+m-1)}{(2n-3)(2n-1)} P_{n-2}^m(\zeta_0) \right. \\ & \quad \left. + \frac{a^{2n-1}}{r_0^{n+1}} (n-1)(n-m) \left(\frac{a^2(2n-1)}{(2n-3)(2n+1)} - \frac{r_0^2}{2(2n-1)} \right) P_n^m(\zeta_0) \right] \\ b_n^m &= \frac{(n-m)!}{(n+m)!} \varepsilon_m \frac{a^{2n+1}}{r_0^{n+1}} \frac{m}{n^2} P_n^m(\zeta_0) \\ c_n^m &= -\frac{1}{2} \frac{(n-m)!}{(n+m)!} \varepsilon_m \frac{a^{2n+3}}{r_0^{n+3}} \frac{(n-1)(n-m+1)(n-m+2)}{(2n+1)(n+m+1)(n+2)} P_{n+2}^m(\zeta_0) \end{aligned} \quad (49)$$

For the purpose of the numerical calculations, the above formulation can be transformed from relationships in Appendix: one develops the three components of $\mathbf{H}_2^S(\mathbf{r})$ as $\sum_{n=1}^{\infty} \sum_{m=0}^n [h_n^m|_r \hat{\mathbf{r}} + h_n^m|_{\zeta} \hat{\boldsymbol{\zeta}} + h_n^m|_{\varphi} \hat{\boldsymbol{\varphi}}]$ the scalar coefficients of which are

$$\begin{aligned} h_n^m|_r &= r^{-(n+2)} \left[(d_n^m + nc_{n-1}^m) r^2 - (n+1)a_{n+1}^m \right] P_n^m(\zeta) \cos[m(\varphi - \varphi_0)], \\ h_n^m|_{\zeta} &= r^{-(n+2)} \left[\frac{m}{\sqrt{1-\zeta^2}} b_n^m r P_n^m(\zeta) - (c_{n-1}^m r^2 + a_{n+1}^m) \sqrt{1-\zeta^2} P_n^{m'}(\zeta) \right] \\ & \quad \cdot \cos[m(\varphi - \varphi_0)], \\ h_n^m|_{\varphi} &= r^{-(n+2)} \left[\sqrt{1-\zeta^2} b_n^m r P_n^{m'}(\zeta) - \frac{m}{\sqrt{1-\zeta^2}} (c_{n-1}^m r^2 + a_{n+1}^m) P_n^m(\zeta) \right] \\ & \quad \cdot \sin[m(\varphi - \varphi_0)], \end{aligned} \quad (50)$$

with possibly further rearrangements for programming convenience.

4. NUMERICAL ILLUSTRATIONS

Numerical results displayed for illustration are obtained in the case of a perfectly conducting sphere of radius $a = 50$ m, centered at the origin O of the co-ordinates system (x_1, x_2, x_3) , and placed in an homogeneous infinite space of $2 \cdot 10^{-4}$ S/m conductivity, when it is illuminated at 500Hz frequency by a vertical magnetic dipole ($\mathbf{M} = M \hat{\mathbf{x}}_3$, $M = 4\pi 10^3$ Am²), localized at $x_1 = 200$ m, $x_2 = 0$, $x_3 = 200$ m in the (x_1, x_3) -plane. The field is evaluated along a probing line parallel to the x_3 -axis (depth) with co-ordinates $x_1 = x_2 = 141.4$ m; only the real (in-phase) part and imaginary (quadrature) parts of the x_2 -component are displayed in Figures 2 and 3, conclusions that can be drawn from the observation of the other components being similar.

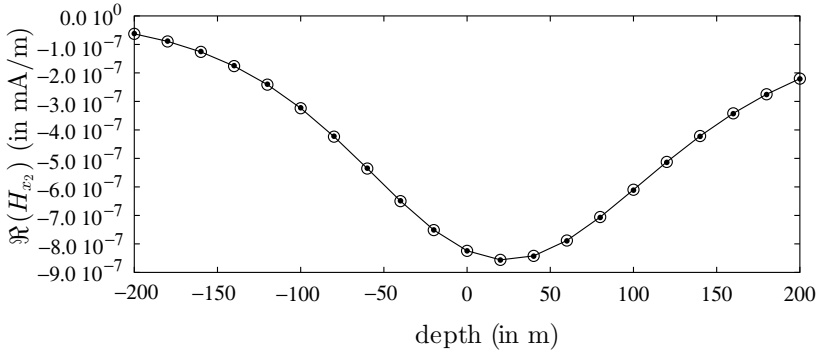


Figure 2. Real part of the secondary magnetic field. It is approximated with the low-frequency series expansion up to order 2 (black dots) and 3 (circles) or calculated via the exact Mie series expansion (solid line).

The approximated field values are calculated from the low-frequency expansion above, up to order 2, i.e., letting $\mathbf{H}^S = \mathbf{H}_0^S + (jk)^2 \mathbf{H}_2^S$, or up to order 3, i.e., letting $\mathbf{H}^S = \mathbf{H}_0^S + (jk)^2 \mathbf{H}_2^S + (jk)^3 \mathbf{H}_3^S$; they are compared to exact field values calculated by means of a Mie series code.^{||} Since all such fields are known in closed form as infinite harmonic expansions, we display the field values reached after carrying out the full summations (in practice, until numerical convergence is observed).

^{||} Mie series expansions of the electromagnetic field scattered by a perfectly conducting sphere involve the well-known regular vector spherical waves (using standard notions) as proper solutions of the Helmholtz vector equation (here to be taken with complex wave number). A good example is found in Tortel's contribution [16] for an electric dipole, and in effect one uses similar (dual) expansions for our magnetic dipole illumination.

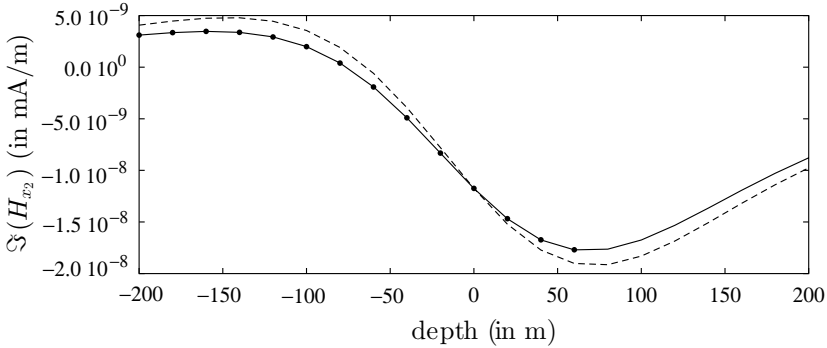


Figure 3. Imaginary part of the scattered magnetic field. It is approximated with the low-frequency series expansion up to order 2 (dashed line) and 3 (black dots) or calculated via the exact Mie series expansion (solid line).

As is evidenced from Figure 2, the in-phase part of the field is perfectly reproduced by means of the low-frequency approach stopped at order 2, and pursuing the expansion up to order 3 does not change anything. This was clearly expected from previous results in [10] since the zero-order term (the static one) yielded the same real-valued field as the Mie series expansion; in short, the third order term of the low-frequency expansion is so small a contributor that it does not add anything useful (as for the second-order term, it is purely imaginary).

For the quadrature part of the field, the potential contributors result from terms at order 2, $(jk)^2 \mathbf{H}_2^S$, and order 3, $(jk)^3 \mathbf{H}_3^S$. In effect, both contributions matter, in contrast with the above where the third-order term is negligible. This is illustrated in figure 3, where the quadrature field values provided by the low-frequency expansion up to order 3 and the exact Mie series ones are shown to fully agree, whereas the order 2 term does not accurately reproduce the exact field.

Similar results have been obtained at other frequencies in the same range, which means that the order 3 of the low-frequency expansion is required for a proper evaluation of the field.

To summarize, the imaginary part of the field is fairly reproduced by the second-order term $(jk)^2 \mathbf{H}_2^S$ but the third one $(jk)^3 \mathbf{H}_3^S$ is necessary to achieve a good accuracy. On the other hand, the static field \mathbf{H}_0^S always suffices to provide the real part of the field, and adding higher-order terms has no interest.

Let us however emphasize that one would need terms of order 4 at higher frequencies: at 5000 Hz in the spherical case considered, for example, exact results are very poorly reproduced by the approximated

ones up to order 3. As for dielectric effects that are at least in theory involved in the terms of order 4 and higher, they can be from practical experience, and as already said, safely discarded as far as one does not reach the MHz range (shallow subsoil probing).

5. CONCLUSION

The numerical results above confirm the adequacy of the low-frequency, closed-form analytic modeling of the perfectly conducting sphere in a conductive medium for a dipolar source which one has reached herein. Generalizations are presently under study.

The case of a non-perfectly-conducting sphere —to tackle low-contrast configurations as for example of interest for probing natural cavities in a subsoil— appears cumbersome but is doable from the available material; one simply has to extend the field coefficients inside the sphere volume via summations of internal vector harmonics (consequently introducing three new sets of vector coefficients), and suitably fit the internal and external expansions of these field coefficients at the sphere surface.

More complicated, and in clear need so as to more effectively deal with metallic ores as well as with artificial metal objects, is the full ellipsoidal case. As already indicated work is in progress [14] toward closed-form analytic expansions of the second-order magnetic field coefficient, the main limitation being that these expansions are incomplete due to the lack of ellipsoidal harmonics of degree higher than 3.

To alleviate these limitations, a way forward may be to tackle single bodies modeled as prolate spheroids (subsequently oblate ones via a simple geometric transformation) by means of spheroidal potential functions since those are reduced to well known associated Legendre functions in the prolate spheroidal system. One is presently considering the first steps into that direction, being reminded that the lack of explicit knowledge of vector spheroidal harmonics forces us to consider vector unknowns instead of the much easier scalar ones as demonstrated here in the spherical case.

APPENDIX A. THE VECTOR SPHERICAL HARMONICS AND ASSOCIATED MATERIAL

Most of the material here is borrowed from [17], and it stays in close accord with contents of well-known reference books [15] and [9]. Let

us consider the spherical coordinate system

$$x_1 = r\sqrt{1 - \zeta^2} \cos \varphi, \quad x_2 = r\sqrt{1 - \zeta^2} \sin \varphi, \quad x_3 = r\zeta, \quad (\text{A1})$$

where $\zeta = \cos \theta$, $-1 \leq \zeta \leq 1$, $0 \leq r < +\infty$, $0 \leq \theta \leq \pi$, $0 \leq \varphi < 2\pi$. The outward unit normal vector to the surface of the sphere $r = a$, is

$$\hat{\mathbf{n}}(a, \zeta, \varphi) = \left(\sqrt{1 - \zeta^2} \cos \varphi, \sqrt{1 - \zeta^2} \sin \varphi, \zeta \right) = \frac{\mathbf{r}(a, \zeta, \varphi)}{a}. \quad (\text{A2})$$

Differential operators ∇ and Δ , read as

$$\nabla = \hat{\mathbf{r}} \frac{\partial}{\partial r} - \frac{\sqrt{1 - \zeta^2}}{r} \hat{\zeta} \frac{\partial}{\partial \zeta} + \frac{1}{r\sqrt{1 - \zeta^2}} \hat{\varphi} \frac{\partial}{\partial \varphi}, \quad (\text{A3})$$

$$\Delta = \frac{1}{r^2} \frac{\partial}{\partial r} \left(r^2 \frac{\partial}{\partial r} \right) + \frac{1}{r^2} \frac{\partial}{\partial \zeta} \left[(1 - \zeta^2) \frac{\partial}{\partial \zeta} \right] + \frac{1}{r^2(1 - \zeta^2)} \frac{\partial^2}{\partial \varphi^2}, \quad (\text{A4})$$

where $\hat{\mathbf{r}}$, $\hat{\zeta}$, $\hat{\varphi}$ are the coordinate unit vectors.

For every nonnegative integer n , there exist $(2n + 1)$ linearly independent spherical surface harmonics Y_n^{ms} , either even (with $s = e$ superscript) or odd (with $s = o$ superscript) with respect to φ , $Y_n^{me}(\hat{\mathbf{r}}) = P_n^m(\zeta) \cos m\varphi$ and $Y_n^{mo}(\hat{\mathbf{r}}) = P_n^m(\zeta) \sin m\varphi$, for $m = 0, 1, \dots, n$, $|\zeta| \leq 1$, $\varphi \in [0, 2\pi)$, which are expressed via first-kind Legendre functions of order m and degree n that are given by

$$P_n^m(\zeta) = \frac{(1 - \zeta^2)^{m/2}}{2^n n!} \frac{d^{n+m}}{d\zeta^{n+m}} (\zeta^2 - 1)^n, \quad |\zeta| < 1. \quad (\text{A5})$$

External solid harmonics accordingly are scalar functions $r^{-(n+1)} Y_n^{ms}(\hat{\mathbf{r}})$ defined from $n = 0$, for $m = 0$ to n , and for $s = e, o$. (One will not need those internal, $r^n Y_n^{ms}(\hat{\mathbf{r}})$.)

Similarly, for every nonnegative integer n , there exist $(2n + 1)$ three-member sets of even and odd vector spherical surface harmonics, $(\mathbf{P}_n^{ms}, \mathbf{B}_n^{ms}, \mathbf{C}_n^{ms})$, such that

$$\mathbf{P}_n^{ms}(\hat{\mathbf{r}}) = \hat{\mathbf{r}} Y_n^{ms}(\hat{\mathbf{r}}), \quad (\text{A6})$$

$$\mathbf{B}_n^{ms}(\hat{\mathbf{r}}) = \frac{1}{\sqrt{n(n+1)}} \left[-\sqrt{1 - \zeta^2} \hat{\zeta} \frac{\partial}{\partial \zeta} + \frac{1}{\sqrt{1 - \zeta^2}} \hat{\varphi} \frac{\partial}{\partial \varphi} \right] Y_n^{ms}(\hat{\mathbf{r}}), \quad (\text{A7})$$

$$\mathbf{C}_n^{ms}(\hat{\mathbf{r}}) = -\frac{1}{\sqrt{n(n+1)}} \hat{\mathbf{r}} \times \left[-\sqrt{1 - \zeta^2} \hat{\zeta} \frac{\partial}{\partial \zeta} + \frac{1}{\sqrt{1 - \zeta^2}} \hat{\varphi} \frac{\partial}{\partial \varphi} \right] Y_n^{ms}(\hat{\mathbf{r}}), \quad (\text{A8})$$

pointwise perpendicular to one another:

$$\mathbf{P}_n^{ms} \cdot \mathbf{C}_n^{ms} = \mathbf{C}_n^{ms} \cdot \mathbf{B}_n^{ms} = \mathbf{B}_n^{ms} \cdot \mathbf{P}_n^{ms} = 0. \quad (\text{A9})$$

Implying their external dependance for brevity (again internal harmonics are not used in the present investigation), the external vector spherical harmonics, from $n = 0$, for $m = 0$ to possibly $n + 1$, and for $s = e, o$, follow as

$$\begin{aligned} \mathbf{N}_n^{ms}(\mathbf{r}) &= \nabla(r^{-n}Y_{n-1}^{ms}(\hat{\mathbf{r}})) \\ &= \sqrt{n(n+1)}r^{-(n+1)}\mathbf{B}_{n-1}^{ms}(\hat{\mathbf{r}}) - nr^{-(n+1)}\mathbf{P}_{n-1}^{ms}(\hat{\mathbf{r}}), \end{aligned} \quad (\text{A10})$$

here defined for $n \geq 1$, $m \leq n - 1$, which comprise both radial parts (the \mathbf{P} surface harmonics) and transverse parts (the \mathbf{B} ones), and are both divergence and curl free;

$$\mathbf{M}_n^{ms}(\mathbf{r}) = \nabla \times (r^{-(n+1)}Y_n^{ms}(\hat{\mathbf{r}})\mathbf{r}) = \sqrt{n(n+1)}r^{-(n+1)}\mathbf{C}_n^{ms}(\hat{\mathbf{r}}), \quad (\text{A11})$$

here defined for $n \geq 1$, $m \leq n$, which are purely transverse and are divergence free, their curls being given by $-n\mathbf{N}_{n+1}^{ms}(\mathbf{r})$; and

$$\begin{aligned} \mathbf{G}_n^{ms}(\mathbf{r}) &= r^{-(2n+1)}\nabla(r^{n+1}Y_{n+1}^{ms}(\hat{\mathbf{r}})) \\ &= \sqrt{(n+1)(n+2)}r^{-(n+1)}\mathbf{B}_{n+1}^{ms}(\hat{\mathbf{r}}) + (n+1)r^{-(n+1)}\mathbf{P}_{n+1}^{ms}(\hat{\mathbf{r}}), \end{aligned} \quad (\text{A12})$$

here defined for $n \geq 0$, $m \leq n + 1$, which again comprise radial and transverse parts, the divergences of which are equal to $-(n+1)(2n+1)r^{-(n+2)}Y_{n+1}^{ms}(\hat{\mathbf{r}})$ and the curls of which are equal to $(2n+1)\mathbf{M}_{n+1}^{ms}(\mathbf{r})$.

Notice at this stage the relationships, to be used in the analysis also, concerning the radial contributions of \mathbf{N}_n^{ms} and \mathbf{G}_n^{ms} :

$$\hat{\mathbf{r}} \cdot \mathbf{N}_n^{ms}(\mathbf{r}) = -nr^{-(n+1)}Y_{n-1}^{ms}(\hat{\mathbf{r}}), \quad (\text{A13})$$

$$\hat{\mathbf{r}} \cdot \mathbf{G}_n^{ms}(\mathbf{r}) = (n+1)r^{-(n+1)}Y_{n+1}^{ms}(\hat{\mathbf{r}}), \quad (\text{A14})$$

the \mathbf{M}_n^{ms} being purely transverse.

Consequently, scattered vector field coefficients $\mathbf{U}(\mathbf{r})$ that should be satisfying outside the sphere the homogeneous vector Laplace equation (i.e., that are belonging to the kernel space of the vector Laplacian) enjoy complete representations of the form

$$\begin{aligned} \mathbf{U}(\mathbf{r}) &= \sum_{n=1}^{\infty} \sum_{m=0}^{n-1} \sum_{s=e,o} a_n^{ms} \mathbf{N}_n^{ms}(\mathbf{r}) + \sum_{n=1}^{\infty} \sum_{m=0}^n \sum_{s=e,o} b_n^{ms} \mathbf{M}_n^{ms}(\mathbf{r}) \\ &\quad + \sum_{n=0}^{\infty} \sum_{m=0}^{n+1} \sum_{s=e,o} c_n^{ms} \mathbf{G}_n^{ms}(\mathbf{r}) \end{aligned} \quad (\text{A15})$$

with properly chosen scalar coefficients according to further relationships to be enforced onto them.

REFERENCES

1. Xiong, Z. and A. C. Tripp, "Electromagnetic scattering of large structures in layered earths using integral equations," *Radio Science*, Vol. 30, 921–929, 1995.
2. Oristaglio, M. L. and B. R. Spies (eds.), *Three Dimensional Electromagnetics*, SEG, Tulsa, 1999.
3. Kaufman, A. A. and G. V. Keller, *Inductive Mining Prospecting*, Elsevier Science, New York, 1985.
4. Bourgeois, B., K. Suignard, and G. Perrusson, "Electric and magnetic dipoles for geometric interpretation of three-component electromagnetic data in geophysics," *Inverse Problems*, Vol. 16, 1225–1262, 2000.
5. Dassios G. and R. E. Kleinman, *Low Frequency Scattering*, Oxford University Press, Oxford, 2000.
6. Perrusson, G., D. Lesselier, M. Lambert, B. Bourgeois, A. Charalambopoulos, and G. Dassios, "Conductive masses in a half-space Earth in the diffusive regime: Fast hybrid modeling of a low-contrast ellipsoid," *IEEE Trans. Geoscie. Remote Sensing*, Vol. 38, 1585–1599, 2000.
7. Habashy, T. M., R. W. Groom, and B. R. Spies, "Beyond the Born and Rytov approximations: A nonlinear approach to electromagnetic scattering," *J. Geophys. Res.*, Vol. 98, 1759–1775, 1993.
8. Charalambopoulos, A., G. Dassios, G. Perrusson, and D. Lesselier, "The localized nonlinear approximation in ellipsoidal geometry: a novel approach to the low frequency problem," *Int. J. Engineer. Scie.*, Vol. 40, 67–91, 2002.
9. Hobson, E. W., *The Theory of Spherical and Ellipsoidal Harmonics*, Chelsea, New York, 1955.
10. Perrusson, G., D. Lesselier, P. Vafeas, G. Kamvyssas, and G. Dassios, "Low-frequency electromagnetic modeling and retrieval of simple orebodies in a conductive Earth," *Progress in Analysis*, H. G. W., R. Begehr, P. Gilbert, and M. W. Wong (eds.), Vol. 2, 1413–1422, World Scientific, London, 2003.
11. Ao, O. C., H. Braunisch, K. O'Neill, and J. A. Kong, "Quasi-magnetostatic solution for a conducting and permeable spheroid

- with arbitrary excitation," *IEEE Trans. Geosci. Remote Sensing*, Vol. 39, 2689–2701, 2001.
12. Bowman, J. J., P. L. Uslenghi, and T. B. Senior (eds.), *Electromagnetic and Acoustic Scattering by Simple Shapes*, J. J. North Holland, Amsterdam, 1969.
 13. Varadan, V. K. and V. V. Varadan (eds.), *Acoustic, Electromagnetic and Elastic Wave Scattering. Low and High Frequency Asymptotics*, North Holland, Amsterdam, 1987.
 14. Perrusson, G., P. Vafeas, and D. Lesselier, "Low-frequency modeling of the interaction of magnetic dipoles and ellipsoidal bodies in a conductive medium," *Proc. 2004 Int. URSI Symp. Electromagn. Theory*, Pisa, May 2004 (to appear).
 15. Morse, P. M. and H. Feshbach, *Methods of Theoretical Physics*, Vols. I, II, McGraw-Hill, New York, 1953.
 16. Tortel, H., "Electromagnetic imaging of a three-dimensional perfectly conducting object using a boundary integral formulation," *Inverse Problems*, Vol. 20, 385–398, 2004.
 17. Dassios, G. and P. Vafeas, "Comparison of differential representations for radially symmetric Stokes flow," *Abstract and Applied Analysis*, 2004 (to appear).

Panayiotis Vafeas was born in Greece in 1974. He received his diploma in Chemical Engineering (1997), his Master of Sciences in Simulation, Optimization and Modulation of Processes (2003) and his Ph.D. in Theory of Differential Representations in Stokes Flow (2003) from the University of Patras, where he has been working, under Professor George Dassios' supervision, in Stokes flow dynamics. He is now engaged in Stokes flow, in electromagnetics and in continuum mechanics. His interests include low frequency scattering in spherical, spheroidal, and ellipsoidal geometry with emphasis on geophysical applications and the use of general mathematical methods in engineering and scientific problems.

Gaële Perrusson was born in France in 1971. She received the degree of Doctorat en Sciences from the Université de Versailles Saint-Quentin in 1999. Since 1996, her research activities have been conducted within the Laboratoire des Signaux et Systèmes (L2S), now joint laboratory of Supélec, Centre National de la Recherche Scientifique and Université Paris Sud, where she is Maître de Conférences since September 2001, and she is also with the Département de Recherche en Electromagnétisme (Supélec-L2S). Her work focuses on

the mathematical modeling and numerical simulation of the interaction of wave fields with buried bodies, with emphasis onto shallow and deep subsurface electromagnetic imaging and inversion. She was the recipient of a Young Scientist Award from URSI in 1998, and she is a member of URSI Commission B.

Dominique Lesselier was born in France in 1953. He received the degree of Engineer from the Ecole Supérieure d'Electricité (now Supélec), Paris, in 1975, and Docteur d'Etat es Sciences Physiques in 1982 from the Université Pierre et Marie Curie, Paris. Since 1975 —as Directeur de recherche CNRS since October 1988— he has been with the Laboratoire des Signaux et Systèmes (L2S), now joint laboratory of Supélec, Centre National de la Recherche Scientifique (CNRS) and Université Paris Sud, and he is also with the Département de Recherche en Electromagnétisme (Supélec-L2S). His main research activity pertains to the development of solution methods of wave field inverse problems, from mathematical theory to numerical solutions to pertinent applications, and vice versa. D. Lesselier is Associate Editor of Radio Science, and is on the Editorial Board of Inverse Problems, the Standing Committee of the Electromagnetic Non-Destructive Evaluation (E'NDE) workshop series and the International Steering Committee of the International Symposia on Applied Electromagnetics and Mechanics (ISEM). Fellow of the Institute of Physics, he is a member of IEEE, the Electromagnetics Academy, and URSI Commission B.